

# Securing UAV Communications via Joint Trajectory and Power Control

Guangchi Zhang, *Member, IEEE*, Qingqing Wu, *Member, IEEE*, Miao Cui,  
Rui Zhang, *Fellow, IEEE*

## Abstract

Unmanned aerial vehicle (UAV) communication is anticipated to be widely applied in the forthcoming fifth-generation (5G) wireless networks, due to its many advantages such as low cost, high mobility, and on-demand deployment. However, the broadcast and line-of-sight (LoS) nature of air-to-ground wireless channels gives rise to a new challenge on how to realize secure UAV communications with the destined nodes on the ground. This paper aims to tackle this challenge by applying the physical (PHY) layer security technique. We consider both the downlink and uplink UAV communications with a ground node, namely UAV-to-ground (U2G) and ground-to-UAV (G2U) communication, respectively, subject to a potential eavesdropper on the ground. In contrast to the existing literature on wireless PHY layer security only with ground nodes at fixed or quasi-static locations, we exploit the high mobility of the UAV to proactively establish favorable and degraded channels for the legitimate and eavesdropping links, respectively, via its trajectory design. We formulate new problems to maximize the average secrecy rates of the U2G and G2U transmissions, respectively, by jointly optimizing the UAV's trajectory and the transmit power of the legitimate transmitter over a given flight period of the UAV. Although the formulated problems are non-convex, we propose iterative algorithms to solve them efficiently by applying the block coordinate descent and successive convex optimization methods. Specifically, the transmit power and UAV trajectory are each optimized with the other being fixed in an alternating manner, until they converge. Simulation results show that the proposed algorithms can improve the secrecy rates for both U2G and G2U communications, as compared to other benchmark schemes without power control and/or trajectory optimization.

G. Zhang and M. Cui are with the School of Information Engineering, Guangdong University of Technology, Guangzhou, China (email: {gc Zhang, cuimiao}@gdut.edu.cn). Q. Wu and R. Zhang are with the Department of Electrical and Computer Engineering, National University of Singapore (email: {elewuqq, elezhang}@nus.edu.sg). Q. Wu is the corresponding author. Part of this paper has been presented in IEEE Global Communications Conference (GLOBECOM), Singapore, Dec. 2017 [1].

## Index Terms

5G and UAV communications, physical layer security, secrecy rate maximization, trajectory design, power control.

### I. INTRODUCTION

With many advantages such as high mobility, low cost, wide coverage, and on-demand deployment, unmanned aerial vehicles (UAVs) have been extensively used in both military and civilian applications, such as search and rescue, inspection and surveillance, cargo transportation, etc. Recently, UAVs have also found increasingly more substantial applications in wireless communication [2], and are expected to play a significant role in the forthcoming fifth-generation (5G) wireless networks. To seize this growing opportunity, internationally leading telecommunication companies such as Qualcomm, Ericsson, and China Mobile have already launched their research projects on integrating UAVs into the 5G networks [3], [4]. Generally speaking, there are two main paradigms of UAV applications in 5G. In the first one, termed as “UAV-assisted wireless communication”, UAVs are utilized as airborne communication platforms such as mobile base stations (BSs) and/or relays that can be flexibly deployed on demand to assist the communications in terrestrial networks such as 5G. For example, UAV-mounted BSs can be used to enable rapid wireless communication service recovery after ground infrastructure damages, or provide offloading service for terrestrial BSs in extremely crowded areas [5]–[11]. Another example is to use UAVs as mobile relays to provide reliable connectivity between distant users in remote areas (e.g., an uninhabited desert) that are not covered by any existing wireless networks [12], [13]. Moreover, in future internet of things (IoT) applications, UAVs can be dispatched to disseminate/collect data to/from widespread distributed wireless devices efficiently and with low cost [14], [15]. By contrast, in the other paradigm, known as “cellular-enabled UAV communication”, UAVs are regarded as new “sky” users in the cellular networks that enable two-way communications of the UAVs with ground BSs. For example, the future 5G networks can provide reliable communications for UAVs even beyond the range of their operators’ visual line-of-sight (LoS) to achieve long-range UAV control in real time [16]. Besides, in UAV-enabled surveillance applications, the captured pictures and/or videos by the UAVs in real time can be uploaded timely to the ground data centers via the 5G networks [17].

In the aforementioned UAV communication applications in 5G, due to the broadcast nature of wireless channels, their security and privacy are of utmost concern [18], [19]. One major

advantage of UAV-ground communications is that UAVs usually have LoS channels for the communications with ground nodes, especially in outdoor environments. However, such LoS communication links are also more prone to the eavesdropping by illegitimate nodes on the ground, which gives rise to a new security challenge. Although security was conventionally viewed as a higher layer communication protocol stack design problem that can be tackled by using cryptographic methods, physical (PHY) layer security has emerged as a promising alternative way of defense to realize secrecy in wireless communication.

A key design metric that has been widely adopted in PHY layer security is the so-called secrecy rate [18]–[25], at which confidential message can be reliably transmitted without having the eavesdropper infer any information about the message. A non-zero secrecy rate can be achieved when the strength of the legitimate link is stronger than that of the eavesdropping link. In the existing literature on PHY layer security, communication nodes are usually assumed to be at fixed or quasi-static locations. As a result, the average channel quality of the legitimate/eavesdropping link mainly depends on the path loss and shadowing from the transmitter to receiver, which are determined if the locations of the legitimate transmitter/receiver and the eavesdropper are given. Thus, in the case that the average channel gain of the legitimate receiver is smaller than that of the eavesdropper (e.g., due to longer distance from the legitimate transmitter), in order to achieve positive secrecy rates, the exploitation of the wireless channel small-scale fading in time, frequency, and/or space becomes essential, and various techniques such as power control in time and/or frequency as well as multi-antenna beamforming have been investigated. In [18], power control with rate adaptation over fading channels is proposed to maximize the average secrecy rate. This work is also extended to characterize the secrecy rate region of parallel-fading broadcast channels [19]. In [20], power control over frequency subcarriers is investigated for secrecy rate maximization in an orthogonal frequency-division multiple access (OFDMA) system. In [21], joint power control on information signal and artificial noise (AN) is proposed to maximize the secrecy rate of a simultaneous wireless information and power transfer (SWIPT) system. In multiple-input multiple-output (MIMO) systems, transmit beamforming can be jointly employed with AN transmission to effectively enhance the legitimate link capacity and at the same time degrade that of the eavesdropping link. For example, the legitimate transmitter can use beamforming to steer a null to the eavesdropper, or send AN in the direction of the eavesdropper to interfere with it [22], [23]. If one or more relay helpers are available, they can also cooperatively send AN or jamming signals to interfere with the eavesdroppers to

achieve better secrecy communication performance. In [24], optimal cooperative jamming via relays is studied to maximize the secrecy rate of a single-antenna point-to-point legitimate link. Besides, transmission scheduling by exploiting multiuser channel diversity is another effective approach to improve the secrecy communication performance in a system with multiple legitimate users/eavesdroppers. In [25], a transmission scheduling scheme is proposed to maximize the secrecy rate of a multiuser cognitive radio network.

However, there are still two major challenges that remain unsolved in the existing PHY layer security literature. First, the practically achievable secrecy rate can be severely limited if the distance between the legitimate transmitter and its intended receiver is fixed and significantly larger than that between it and a potential eavesdropper, even if the various approaches mentioned above are applied. Second, the channel state information (CSI) of the eavesdropper is usually required at the legitimate transmitter for the implementation of effective power control and/or beamforming techniques. This is practically challenging since the eavesdropper is usually a passive device and thus it is difficult to estimate such CSI. In this paper, we study PHY layer security in UAV-ground communications, which may potentially overcome the above two critical issues in conventional studies. First, in contrast to the existing literature with fixed or quasi-static nodes only, the high mobility of UAVs can be exploited to proactively establish stronger links with the legitimate ground nodes and/or degrade the channels of the eavesdroppers, by flying closer/farther to/from them, respectively, via proper trajectory design. This approach is particularly effective in the context of UAV-ground communications (as compared to conventional terrestrial communications), since the LoS links are usually much more dominant over other channel impairments such as shadowing and small-scale fading, due to the much larger height of the UAV than typical ground nodes such as mobile terminals or BSs. Furthermore, since the LoS channel gain is only determined by the link distance, the UAV can practically obtain the channel gain to any potential eavesdropper on the ground if its location is known, which thus resolves the eavesdropper-CSI issue in the existing literature. Note that the location of any ground node as a potential eavesdropper can be practically detected and tracked by the UAV via using an optical camera or synthetic aperture radar (SAR) equipped on the UAV [26], [27].

For an initial exposition, in this paper we consider a simplified three-node secrecy UAV-ground communication system as shown in Fig. 1, where a UAV at fixed altitude intends to communicate with a ground node, while a potential eavesdropper on the ground may intercept their communication. The secure communications of both UAV-to-ground (U2G) and ground-

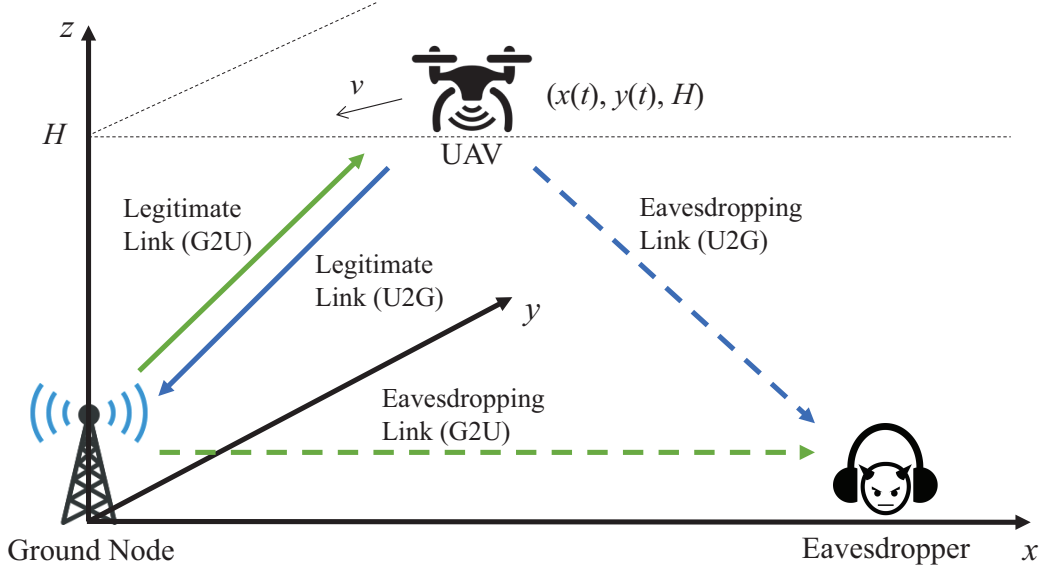


Fig. 1. A UAV wireless communication system consisting of a UAV above ground and a node on the ground. A potential eavesdropper on the ground intends to intercept the wireless communication between them.

to-UAV (G2U) links are considered. In the U2G case, the UAV and the ground node are the legitimate transmitter and receiver, respectively, where both the legitimate and eavesdropping links are modeled as LoS channels. By contrast, in the G2U case, the ground node and the UAV are the legitimate transmitter and receiver, respectively. Since the legitimate transmitter and potential eavesdropper are both on the ground in this case, different from the U2G case, only the legitimate link is modeled as a LoS channel, while the eavesdropping link is practically modeled as a channel consisting of both distance-dependent path-loss and small-scale Rayleigh fading. Thus, the problem formulations for the secrecy rate maximization in these two cases are generally different, which will be detailed later in this paper. Nevertheless, the secrecy rates of both U2G and G2U transmissions can benefit from the joint design of UAV trajectory and transmit power control at the legitimate transmitter (i.e., UAV and ground node in the U2G and G2U cases, respectively), explained as follows. On one hand, the location of the UAV can be adjusted dynamically to establish stronger channels for the legitimate link than that for the eavesdropping link. On the other hand, due to practical constraints such as the UAV's initial and final locations, the legitimate link may not be always stronger than the eavesdropping link during the whole flight period of the UAV. In this case, transmit power can be adapted to the channel variations arising from the UAV's movement to further improve the secrecy rate. For example,

in the U2G case, the UAV should transmit higher power when it flies closer to the ground node while being more far away from the eavesdropper, and transmit lower or zero power otherwise.

Motivated by this, we aim to design joint UAV trajectory and transmit power optimization algorithms to secure both U2G and G2U communications. Our goal is to maximize the average secrecy rate over a finite flight period of the UAV in each case, subject to the practical mobility constraints on the UAV's maximum speed and its initial and final locations, as well as the average and peak transmit power constraints. For the U2G case, the formulated joint trajectory and power control problem for average secrecy rate maximization is difficult to be solved directly due to its non-smooth objective function. To tackle this difficulty, we reformulate the problem into an equivalent problem with a smooth objective function without loss of optimality. Although the non-smoothness issue is resolved, the reformulated problem is still non-convex due to the coupling of the transmit power and UAV trajectory optimization variables. We thus propose an efficient iterative algorithm for solving this problem approximately based on the block coordinate descent method. Specifically, we divide the optimization variables into two blocks, one for transmit power control and the other for UAV trajectory optimization. Then the two blocks of variables are optimized alternately in an iterative manner, i.e., in each iteration one block is optimized with the other block fixed and vice versa. One corresponding sub-problem that optimizes the UAV trajectory under given transmit power is still difficult to solve due to its non-convexity. We thus apply the successive convex optimization method to solve the problem approximately. Finally, we show that our proposed joint optimization algorithm is guaranteed to converge. On the other hand, for the G2U case, similar to the U2G case, we also propose an efficient algorithm to solve the formulated problem by using the block coordinate descent and successive convex optimization methods, while some modification is made in the problem formulation to deal with the non-LoS channel of the eavesdropper link in this case. Simulation results show that the proposed joint trajectory and transmit power designs can improve the average secrecy rates in both U2G and G2U communications, as compared to other benchmark schemes without applying the trajectory optimization and/or transmit power control. Furthermore, it is observed that trajectory optimization and transmit power control are both essential for the U2G case, while for the G2U case, trajectory optimization is less effective as compared to power control.

It is worth noting that there have been prior works (e.g. [9], [12], [28], [29]) on trajectory optimization for various UAV communication systems, which consider different system setups and design objectives. In [9], a UAV mobile BS serving multiple users is considered, where

the UAV trajectory and multiuser scheduling are jointly designed to maximize the minimum throughput of the users. In [12], a UAV-enabled mobile relaying system is investigated, where the UAV trajectory and transmit power are jointly designed to maximize the throughput. In [28], the UAV flying heading is optimized to maximize the achievable sum rate from ground nodes to a UAV by assuming a constant flying speed. In [29], a new design paradigm that jointly considers both the communication throughput and the UAV's flying energy consumption is proposed to maximize the energy efficiency of a point-to-point U2G communication system. Different from these prior works, in this paper, we apply both trajectory optimization and transmit power control to maximize the secrecy rates of both U2G and G2U communications.

The remainder of this paper is organized as follows. Section II presents the system model and problem formulation. Sections III and IV present joint trajectory optimization and transmit power control algorithms for the U2G and G2U cases, respectively. Section V provides simulation results to validate the performance of the proposed algorithms as compared to three benchmark schemes. Finally, Section VI concludes the paper.

## II. SYSTEM MODEL AND PROBLEM FORMULATION

### A. System Model

As shown in Fig. 1, we consider a UAV-enabled wireless communication system where a UAV above ground and a node on the ground communicate with each other, while a potential eavesdropper on the ground aims to intercept the communications between them. We assume that the distance between the ground node and the potential eavesdropper is  $L$  meters (m). Without loss of generality, we consider a three-dimensional (3D) Cartesian coordinate system with the ground node and the eavesdropper located at  $(0, 0, 0)$  and  $(L, 0, 0)$  in m, respectively. Their locations are assumed to be fixed and known to the UAV, where the location of the eavesdropper can be detected by using an optical camera or SAR equipped on the UAV. On the other hand, the obtained secrecy rate when the location of the eavesdropper is known serves as an upper bound for that when the location of the eavesdropper is not known.

We consider a given finite flight period of the UAV, with the duration denoted by  $T$  in seconds (s). It is assumed that the UAV flies at a fixed altitude of  $H$  in m above ground, which can be considered as the minimum altitude required for safety considerations such as terrain or building avoidance. The coordinate of the UAV over time is denoted as  $(x(t), y(t), H)$  in m,  $0 \leq t \leq T$ . For convenience, we divide the period  $T$  into  $N$  time slots with equal length, i.e.,  $T = Nd_t$ , with

$d_t$  in s denoting the length of a time slot, which is chosen sufficiently small such that the UAV's location can be regarded as unchanged within each time slot from the viewpoint of the ground node. As a result, the UAV's coordinate in slot  $n$  can be denoted as  $(x[n], y[n], H)$ , and the UAV's horizontal trajectory  $(x(t), y(t))$  over the flight period  $T$  can be approximated by the sequence  $\{x[n], y[n]\}_{n=1}^N$ . Denote the maximum speed of the UAV as  $v_{\max}$  in m/s. Thus, the maximum flying distance of the UAV in each slot is  $D = v_{\max}d_t$ . The initial and final locations of the UAV are assumed to be given, which are denoted by  $(x_0, y_0, H)$  and  $(x_F, y_F, H)$  in m, respectively. For the UAV trajectory to be feasible, we assume that the distance between the initial and final location satisfies that  $\sqrt{(x_F - x_0)^2 + (y_F - y_0)^2} \leq v_{\max}T$ . As a result, the mobility constraints of the UAV can be expressed as

$$(x[1] - x_0)^2 + (y[1] - y_0)^2 \leq D^2, \quad (1a)$$

$$(x[n+1] - x[n])^2 + (y[n+1] - y[n])^2 \leq D^2, \quad n = 1, \dots, N-1, \quad (1b)$$

$$(x_F - x[N])^2 + (y_F - y[N])^2 \leq D^2. \quad (1c)$$

We consider both the U2G and G2U communications in the system of interest, which are specified in detail in the following, respectively.

1) *U2G Transmission*: In the U2G case, the UAV and the ground node play the roles of legitimate transmitter and receiver, respectively. The legitimate link from the UAV to the ground node and the eavesdropping link from the UAV to the eavesdropper are both assumed to be LoS channels. The measurement results in [30] have shown that the LoS model offers a good approximation for practical UAV-ground communications. Thus, the LoS channel power gain from the UAV to the ground node in time slot  $n$  follows the free-space path loss model, given by

$$g_{\text{UG}}[n] = \beta_0 d_{\text{UG}}^{-2}[n] = \frac{\beta_0}{x^2[n] + y^2[n] + H^2}, \quad (2)$$

where  $\beta_0$  denotes the channel power gain at the reference distance  $d_0 = 1\text{m}$ , which depends on the carrier frequency and the antenna gains of the transmitter and receiver, and  $d_{\text{UG}}[n] = \sqrt{x^2[n] + y^2[n] + H^2}$  is the distance from the UAV to the ground node in time slot  $n$ . Similarly, the LoS channel power gain from the UAV to the eavesdropper in time slot  $n$  is given by

$$g_{\text{UE}}[n] = \frac{\beta_0}{(x[n] - L)^2 + y^2[n] + H^2}. \quad (3)$$



We denote  $p[n]$  as the transmit power of the UAV in time slot  $n$ . In practice,  $p[n]$ 's are usually subject to both average and peak limits over time, denoted by  $\bar{P}$  and  $P_{\text{peak}}$ , respectively. Thus, the transmit power constraints are expressed as

$$\frac{1}{N} \sum_{n=1}^N p[n] \leq \bar{P}, \quad (4a)$$

$$0 \leq p[n] \leq P_{\text{peak}}, \quad \forall n. \quad (4b)$$

To make the constraint in (4a) non-trivial, we assume  $\bar{P} < P_{\text{peak}}$  in this paper. In the absence of the eavesdropper, the achievable rate from the UAV to the ground node in bits/second/Hertz (bps/Hz) in time slot  $n$  can be expressed as

$$\begin{aligned} R_{\text{UG}}[n] &= \log_2 \left( 1 + \frac{p[n]g_{\text{UG}}[n]}{\sigma^2} \right) \\ &= \log_2 \left( 1 + \frac{\gamma_0 p[n]}{x^2[n] + y^2[n] + H^2} \right), \end{aligned} \quad (5)$$

where  $\sigma^2$  is the additive white Gaussian noise (AWGN) power at the receiver and  $\gamma_0 = \beta_0/\sigma^2$  is the reference signal-to-noise ratio (SNR). Similarly, the achievable rate from the UAV to the eavesdropper in bps/Hz in time slot  $n$  is given by

$$R_{\text{UE}}[n] = \log_2 \left( 1 + \frac{\gamma_0 p[n]}{(x[n] - L)^2 + y^2[n] + H^2} \right). \quad (6)$$

With (5) and (6), the average secrecy rate achievable for the U2G link in bps/Hz over the total  $N$  time slots is given by [18]

$$R_{\text{sec}}^{(\text{U2G})} = \frac{1}{N} \sum_{n=1}^N \left[ \log_2 \left( 1 + \frac{\gamma_0 p[n]}{x^2[n] + y^2[n] + H^2} \right) - \log_2 \left( 1 + \frac{\gamma_0 p[n]}{(x[n] - L)^2 + y^2[n] + H^2} \right) \right]^+, \quad (7)$$

where  $[x]^+ \triangleq \max(x, 0)$ .

2) *G2U Transmission*: In the G2U case, the ground node and the UAV play the roles of legitimate transmitter and receiver, respectively. The legitimate channel from the ground node to the UAV is assumed to be LoS, similar as in the U2G case, whose channel power gain in time slot  $n$  is given by

$$g_{\text{GU}}[n] = \frac{\beta_0}{x^2[n] + y^2[n] + H^2}. \quad (8)$$

Since both the ground node and the eavesdropper are on the ground, the eavesdropping channel between them is assumed to constitute both distance-dependent path loss with pass-loss exponent

$\kappa \geq 2$  and small-scale Rayleigh fading. Thus, the channel power gain from the ground node to the eavesdropper at any time is given by

$$g_{\text{GE}} = \frac{\beta_0}{L^\kappa} \zeta, \quad (9)$$

where  $\zeta$  is an exponentially distributed random variable with unit mean accounting for the Rayleigh fading.

We denote  $q[n]$  as the transmit power of the ground node in time slot  $n$ . Similar to the U2G case,  $q[n]$ 's are constrained by average power limit  $\bar{Q}$  and peak power limit  $Q_{\text{peak}}$ , i.e.,

$$\frac{1}{N} \sum_{n=1}^N q[n] \leq \bar{Q}, \quad (10a)$$

$$0 \leq q[n] \leq Q_{\text{peak}}, \quad \forall n, \quad (10b)$$

where  $\bar{Q} < Q_{\text{peak}}$  is assumed. Similar to (5), the achievable rate from the ground node to the UAV in bps/Hz in time slot  $n$  can be expressed as

$$R_{\text{GU}}[n] = \log_2 \left( 1 + \frac{\gamma_0 q[n]}{x^2[n] + y^2[n] + H^2} \right). \quad (11)$$

The achievable rate from the ground node to the eavesdropper in bps/Hz in time slot  $n$  is expressed as

$$R_{\text{GE}}[n] = \mathbb{E}_\zeta \left[ \log_2 \left( 1 + \frac{\gamma_0 q[n]}{L^\kappa} \zeta \right) \right] \quad (12a)$$

$$\leq \log_2 \left( 1 + \frac{\gamma_0 q[n]}{L^\kappa} \mathbb{E}_\zeta [\zeta] \right) \quad (12b)$$

$$= \log_2 \left( 1 + \frac{\gamma_0 q[n]}{L^\kappa} \right), \quad (12c)$$

where  $\mathbb{E}_\zeta[\cdot]$  in (12a) denotes the mathematical expectation with respect to random variable  $\zeta$ , and the inequality in (12b) is due to Jensen's inequality and the fact that  $\log_2(1 + \gamma_0 q[n] \zeta / L^\kappa)$  is concave with respect to  $\zeta$ . (12c) shows an upper bound of  $R_{\text{GE}}[n]$ . We consider the worst-case secrecy rate performance by assuming that the eavesdropper is able to achieve this upper bound. With (11) and (12c), the following average secrecy rate of the G2U link in bps/Hz over the total  $N$  time slots is thus achievable,

$$R_{\text{sec}}^{(\text{G2U})} = \frac{1}{N} \sum_{n=1}^N \left[ \log_2 \left( 1 + \frac{\gamma_0 q[n]}{x^2[n] + y^2[n] + H^2} \right) - \log_2 \left( 1 + \frac{\gamma_0 q[n]}{L^\kappa} \right) \right]^+. \quad (13)$$

## B. Problem Formulation

For the U2G case, our goal is to maximize the average secrecy rate  $R_{\text{sec}}^{(\text{U2G})}$  in (7) by jointly optimizing the UAV's transmit power  $\mathbf{p} \triangleq [p[1], \dots, p[N]]^\dagger$  and the UAV's trajectory in terms of its horizontal coordinates  $\mathbf{x} \triangleq [x[1], \dots, x[N]]^\dagger$  and  $\mathbf{y} \triangleq [y[1], \dots, y[N]]^\dagger$  over all the  $N$  time slots, where the superscript  $\dagger$  denotes the transpose operation. The optimization variables are subject to the UAV's mobility constraints in (1) and the average and peak transmit power constraints in (4). We formulate the secrecy rate maximization problem as follows (by dropping the constant term  $1/N$  in (7))

$$\begin{aligned} \text{(P1)} : \max_{\mathbf{x}, \mathbf{y}, \mathbf{p}} \sum_{n=1}^N & \left[ \log_2 \left( 1 + \frac{\gamma_0 p[n]}{x^2[n] + y^2[n] + H^2} \right) \right. \\ & \left. - \log_2 \left( 1 + \frac{\gamma_0 p[n]}{(x[n] - L)^2 + y^2[n] + H^2} \right) \right]^+ \quad (14) \\ \text{s.t.} & \text{ (1), (4).} \end{aligned}$$

Similarly, for the G2U case, we maximize  $R_{\text{sec}}^{(\text{G2U})}$  in (13) by jointly optimizing the ground node's transmit power  $\mathbf{q} \triangleq [q[1], \dots, q[N]]^\dagger$  and the UAV's horizontal trajectory  $\mathbf{x}$  and  $\mathbf{y}$ . The problem is thus formulated as

$$\begin{aligned} \text{(P2)} : \max_{\mathbf{x}, \mathbf{y}, \mathbf{q}} \sum_{n=1}^N & \left[ \log_2 \left( 1 + \frac{\gamma_0 q[n]}{x^2[n] + y^2[n] + H^2} \right) - \log_2 \left( 1 + \frac{\gamma_0 q[n]}{L^\kappa} \right) \right]^+ \quad (15) \\ \text{s.t.} & \text{ (1), (10).} \end{aligned}$$

Note that different from problem (P1), only the first logarithmic function in the objective of (P2), i.e.,  $\log_2 \left( 1 + \frac{\gamma_0 q[n]}{x^2[n] + y^2[n] + H^2} \right)$ , contains the UAV trajectory variables. This is because the achievable rate from the ground node to the eavesdropper does not depend on the trajectory of the UAV.

Problems (P1) and (P2) are both difficult to be solved optimally due to the following two reasons. First, the operator  $[\cdot]^+$  makes the objective functions of (P1) and (P2) non-smooth at zero value. Second, even without  $[\cdot]^+$ , their objective functions are non-concave with respect to either  $\mathbf{x}$ ,  $\mathbf{y}$ , or  $\mathbf{p}$ . In Sections III and IV, we propose efficient algorithms for solving problems (P1) and (P2) approximately, respectively.

## III. PROPOSED ALGORITHM FOR PROBLEM (P1)

First, we consider problem (P1) for the U2G case. To handle the non-smoothness of the objective function of (P1), the following lemma is used.

**Lemma 1.** Problem (P1) has the same optimal value as that of the following problem,

$$\begin{aligned}
 \text{(P3)} : \max_{\mathbf{x}, \mathbf{y}, \mathbf{p}} \sum_{n=1}^N & \left[ \log_2 \left( 1 + \frac{\gamma_0 p[n]}{x^2[n] + y^2[n] + H^2} \right) \right. \\
 & \left. - \log_2 \left( 1 + \frac{\gamma_0 p[n]}{(x[n] - L)^2 + y^2[n] + H^2} \right) \right] \quad (16) \\
 \text{s.t.} & \text{ (1), (4)}.
 \end{aligned}$$

*Proof.* Denote  $L_1$  and  $L_3$  as the optimal values of (P1) and (P3), respectively. First, we have  $L_1 \geq L_3$ , since the objective function of (P1) is no smaller than that of (P3), and (P1) and (P3) have the same constraints.

Next, we show  $L_3 \geq L_1$  also holds. Denote  $(\mathbf{x}^*, \mathbf{y}^*, \mathbf{p}^*)$  as the optimal solution to (P1), where  $\mathbf{x}^* = [x^*[1], \dots, x^*[N]]^\dagger$ ,  $\mathbf{y}^* = [y^*[1], \dots, y^*[N]]^\dagger$ , and  $\mathbf{p}^* = [p^*[1], \dots, p^*[N]]^\dagger$ . Define

$$f(x[n], y[n], p[n]) = \log_2 \left( 1 + \frac{\gamma_0 p[n]}{x^2[n] + y^2[n] + H^2} \right) - \log_2 \left( 1 + \frac{\gamma_0 p[n]}{(x[n] - L)^2 + y^2[n] + H^2} \right).$$

We construct a feasible solution to (P3), termed  $(\tilde{\mathbf{x}}, \tilde{\mathbf{y}}, \tilde{\mathbf{p}})$ , such that  $\tilde{\mathbf{x}} = \mathbf{x}^*$ ,  $\tilde{\mathbf{y}} = \mathbf{y}^*$ , and the elements of  $\tilde{\mathbf{p}}$  are obtained as

$$\tilde{p}[n] = \begin{cases} p^*[n] & f(x^*[n], y^*[n], p^*[n]) \geq 0, \\ 0 & f(x^*[n], y^*[n], p^*[n]) < 0. \end{cases}$$

Denote  $\tilde{L}$  as the objective value of (P3) attained at  $(\tilde{\mathbf{x}}, \tilde{\mathbf{y}}, \tilde{\mathbf{p}})$ . The newly constructed solution  $(\tilde{\mathbf{x}}, \tilde{\mathbf{y}}, \tilde{\mathbf{p}})$  ensures that  $\tilde{L} = L_1$ . Since  $(\tilde{\mathbf{x}}, \tilde{\mathbf{y}}, \tilde{\mathbf{p}})$  is a feasible solution to (P3), it follows that  $L_3 \geq \tilde{L}$ , and thus  $L_3 \geq L_1$ . Therefore,  $L_1 = L_3$ , which completes the proof.  $\square$

Based on Lemma 1, we only need to focus on solving problem (P3). Although problem (P3) resolves the non-smoothness issue, it is still non-convex and difficult to solve. However, we observe that the constraint (1) contains only the variables  $(\mathbf{x}, \mathbf{y})$  for UAV trajectory optimization and the constraint (4) contains only the variables  $\mathbf{p}$  for transmit power control. As such, the optimization variables of (P3) can be partitioned into two blocks, i.e.,  $\mathbf{p}$  and  $(\mathbf{x}, \mathbf{y})$ , respectively, which facilitates the development of an iterative algorithm for solving problem (P3) by applying the block coordinate descent method. Specifically, we solve problem (P3) by solving the following two sub-problems iteratively: one (denoted by sub-problem 1) optimizes the transmit power  $\mathbf{p}$  under given UAV trajectory  $(\mathbf{x}, \mathbf{y})$ , while the other (denoted by sub-problem 2) optimizes the UAV trajectory  $(\mathbf{x}, \mathbf{y})$  under given transmit power  $\mathbf{p}$ , as detailed in the next two subsections, respectively. Then, we present the overall algorithm and show that it is guaranteed to converge.

### A. Sub-Problem 1: Optimizing Transmit Power Given UAV Trajectory

For given UAV trajectory  $(\mathbf{x}, \mathbf{y})$ , sub-problem 1 can be expressed as

$$\begin{aligned} \max_{\mathbf{p}} \quad & \sum_{n=1}^N [\log_2(1 + a_n p[n]) - \log_2(1 + b_n p[n])] \\ \text{s.t.} \quad & (4), \end{aligned} \quad (17)$$

where

$$a_n = \frac{\gamma_0}{x^2[n] + y^2[n] + H^2}, \quad (18)$$

$$b_n = \frac{\gamma_0}{(x[n] - L)^2 + y^2[n] + H^2}. \quad (19)$$

Although problem (17) is non-convex, it has been shown in [18] that the optimal solution can be obtained as

$$p^*[n] = \begin{cases} \min([\hat{p}[n]]^+, P_{\text{peak}}) & a_n > b_n, \\ 0 & a_n \leq b_n, \end{cases} \quad (20)$$

where

$$\hat{p}[n] = \sqrt{\left(\frac{1}{2b_n} - \frac{1}{2a_n}\right)^2 + \frac{1}{\lambda \ln 2} \left(\frac{1}{b_n} - \frac{1}{a_n}\right)} - \frac{1}{2b_n} - \frac{1}{2a_n}. \quad (21)$$

In (21),  $\lambda \geq 0$  is a constant that ensures the average power constraint  $\frac{1}{N} \sum_{n=1}^N p[n] \leq \bar{P}$  to be satisfied when the optimal solution of problem (17) is attained, which can be found efficiently via a one-dimensional bisection search [31].

### B. Sub-Problem 2: Optimizing UAV Trajectory Given Transmit Power

For given transmit power  $\mathbf{p}$ , by letting  $P_n = \gamma_0 p[n]$ , we can express sub-problem 2 as

$$\begin{aligned} \max_{\mathbf{x}, \mathbf{y}} \quad & \sum_{n=1}^N \left[ \log_2 \left( 1 + \frac{P_n}{x^2[n] + y^2[n] + H^2} \right) \right. \\ & \left. - \log_2 \left( 1 + \frac{P_n}{(x[n] - L)^2 + y^2[n] + H^2} \right) \right] \end{aligned} \quad (22)$$

s.t. (1).

Note that the objective function of problem (22) is non-concave with respect to  $\mathbf{x}$  and  $\mathbf{y}$ , so it is a non-convex optimization problem and cannot be solved optimally in general. By introducing

slack variables  $\mathbf{t} = [t[1], \dots, t[N]]^\dagger$  and  $\mathbf{u} = [u[1], \dots, u[N]]^\dagger$ , we first consider the following problem,

$$\max_{\mathbf{x}, \mathbf{y}, \mathbf{t}, \mathbf{u}} \sum_{n=1}^N \left[ \log_2 \left( 1 + \frac{P_n}{u[n]} \right) - \log_2 \left( 1 + \frac{P_n}{t[n]} \right) \right] \quad (23a)$$

$$\text{s.t. } t[n] - x^2[n] + 2Lx[n] - L^2 - y^2[n] - H^2 \leq 0, \quad \forall n, \quad (23b)$$

$$x^2[n] + y^2[n] + H^2 - u[n] \leq 0, \quad \forall n, \quad (23c)$$

$$t[n] \geq H^2, \quad \forall n, \quad (23d)$$

(1).

At the optimal solution of problem (23), constraints (23b) and (23c) should hold with equalities, since otherwise  $t[n]$  ( $u[n]$ ) can be increased (decreased) to improve the objective value. Therefore, problems (22) and (23) have the same optimal solution of  $(\mathbf{x}, \mathbf{y})$ . Next, we focus on solving problem (23).

The term  $\log_2 \left( 1 + \frac{P_n}{u[n]} \right)$  in (23a) is convex with respect to  $u[n]$ , and the terms  $-x^2[n]$  and  $-y^2[n]$  in (23b) are concave with respect to  $x[n]$  and  $y[n]$ , respectively. However, a maximization problem with a non-concave objective function and/or a non-convex feasible region is in general non-convex and thus difficult to be solved optimally. Based on the facts that the first-order Taylor expansion of a convex function is its global under-estimator and that of a concave function is its global over-estimator [31], we propose an iterative algorithm to solve problem (23) approximately by applying the successive convex optimization method. The algorithm obtains an approximate solution to problem (23) by maximizing a concave lower bound of its objective function within a convex feasible region, which is detailed as follows. First, the algorithm assumes a given initial point  $(\mathbf{x}_{\text{fea}}, \mathbf{y}_{\text{fea}}, \mathbf{u}_{\text{fea}})$  which is feasible to (23), where  $\mathbf{x}_{\text{fea}} \triangleq [x_{\text{fea}}[1], \dots, x_{\text{fea}}[N]]^\dagger$ ,  $\mathbf{y}_{\text{fea}} \triangleq [y_{\text{fea}}[1], \dots, y_{\text{fea}}[N]]^\dagger$ , and  $\mathbf{u}_{\text{fea}} \triangleq [u_{\text{fea}}[1], \dots, u_{\text{fea}}[N]]^\dagger$ . Then, by using the first-order Taylor expansions of  $\log_2 \left( 1 + \frac{P_n}{u[n]} \right)$ ,  $-x^2[n]$ , and  $-y^2[n]$  at the points  $u_{\text{fea}}[n]$ ,  $x_{\text{fea}}[n]$ , and  $y_{\text{fea}}[n]$ , respectively, i.e.,

$$\log_2 \left( 1 + \frac{P_n}{u[n]} \right) \geq \log_2 \left( 1 + \frac{P_n}{u_{\text{fea}}[n]} \right) - \frac{P_n(u[n] - u_{\text{fea}}[n])}{\ln 2(u_{\text{fea}}^2[n] + P_n u_{\text{fea}}[n])}, \quad (24)$$

$$-x^2[n] \leq x_{\text{fea}}^2[n] - 2x_{\text{fea}}[n]x[n], \quad (25)$$

$$-y^2[n] \leq y_{\text{fea}}^2[n] - 2y_{\text{fea}}[n]y[n], \quad (26)$$

problem (23) is approximated as

$$\max_{\mathbf{x}, \mathbf{y}, \mathbf{t}, \mathbf{u}} \sum_{n=1}^N \left[ -\frac{P_n u[n]}{\ln 2(u_{\text{fea}}^2[n] + P_n u_{\text{fea}}[n])} - \log_2 \left( 1 + \frac{P_n}{t[n]} \right) \right] \quad (27a)$$

$$\begin{aligned} \text{s.t. } & t[n] + x_{\text{fea}}^2[n] - 2x_{\text{fea}}[n]x[n] + 2Lx[n] - L^2 \\ & + y_{\text{fea}}^2[n] - 2y_{\text{fea}}[n]y[n] - H^2 \leq 0, \quad \forall n, \end{aligned} \quad (27b)$$

(1), (23c), (23d).

After such approximation, we note that the objective function of problem (27) is concave and its feasible region is convex. Thus, problem (27) is a convex optimization problem, which can be optimally solved by the interior-point method [31]. Since the first-order Taylor expansions of  $-x^2[n]$  and  $-y^2[n]$  are their global over-estimators, any solution  $(x[n], y[n])$  satisfying (27b) will satisfy (23b). As a result, the solution of problem (27) is guaranteed to be a feasible solution of problem (23). Moreover, the first-order Taylor expansion of  $\log_2 \left( 1 + \frac{P_n}{u[n]} \right)$  is its global under-estimator. As such, problem (27) maximizes a lower bound of the objective function of problem (23), and the lower bound and the objective function of (23) are equal only at the given point  $(\mathbf{x}_{\text{fea}}, \mathbf{y}_{\text{fea}}, \mathbf{u}_{\text{fea}})$ ; thus, the objective value of problem (23) with the solution obtained by solving problem (27) is no smaller than that with the given point  $(\mathbf{x}_{\text{fea}}, \mathbf{y}_{\text{fea}}, \mathbf{u}_{\text{fea}})$ .

### C. Overall Algorithm

In summary, the overall algorithm applies the block coordinate descent method, and solves the two sub-problems (17) and (27) alternately in an iterative manner. The details of the proposed algorithm are summarized in Algorithm 1. As shown in the previous two subsections, the objective value of (P3) with the solutions obtained by solving the sub-problems (17) and (27) is non-decreasing over iterations, while the optimal value of (P3) is finite; thus, the solution by the proposed algorithm is guaranteed to converge.

## IV. PROPOSED ALGORITHM FOR PROBLEM (P2)

In this section, we consider problem (P2) for the G2U case. Similar to (P1), we solve problem (P2) by considering the following equivalent problem,

$$(\text{P4}) : \max_{\mathbf{x}, \mathbf{y}, \mathbf{q}} \sum_{n=1}^N \left[ \log_2 \left( 1 + \frac{\gamma_0 q[n]}{x^2[n] + y^2[n] + H^2} \right) - \log_2 \left( 1 + \frac{\gamma_0 q[n]}{L^\kappa} \right) \right] \quad (28)$$

s.t. (1), (10).

---

**Algorithm 1** Proposed Algorithm for Problem (P1).

---

- 1: **Initialization:** Set an initial feasible solution  $(\mathbf{p}^{(0)}, \mathbf{x}^{(0)}, \mathbf{y}^{(0)})$ , an initial slack variable  $\mathbf{u}^{(0)}$  and  $k = 0$ .
  - 2: **repeat**
  - 3:   Set  $k \leftarrow k + 1$ ;
  - 4:   With given  $\mathbf{p}^{(k-1)}$ , set the feasible solution  $\mathbf{x}_{\text{fea}} = \mathbf{x}^{(k-1)}$ ,  $\mathbf{y}_{\text{fea}} = \mathbf{y}^{(k-1)}$  and  $\mathbf{u}_{\text{fea}} = \mathbf{u}^{(k-1)}$ , then update the trajectory variable  $(\mathbf{x}^{(k)}, \mathbf{y}^{(k)})$  and the slack variable  $\mathbf{u}^{(k)}$  by solving problem (27);
  - 5:   With given  $(\mathbf{x}^{(k)}, \mathbf{y}^{(k)})$ , update the transmit power control variable  $\mathbf{p}^{(k)}$  by using (20).
  - 6: **until** the fractional increase of the objective value is below a small threshold  $\epsilon$ .
- 

Although problem (P4) is non-convex, it has a similar structure as problem (P3), which facilitates us to also apply the block coordinate descent method to find an approximate solution for it. Like (P3), problem (P4) can also be decomposed into two sub-problems: one (denoted by sub-problem 3) is to optimize transmit power  $\mathbf{q}$  under given trajectory  $(\mathbf{x}, \mathbf{y})$ ; while the other (denoted by sub-problem 4) is to optimize trajectory  $(\mathbf{x}, \mathbf{y})$  under given transmit power  $\mathbf{q}$ . The two sub-problems are solved alternately in an iterative manner until convergence. Next, we discuss on how to solve the two sub-problems, respectively.

#### A. Sub-Problem 3: Optimizing Transmit Power Given UAV Trajectory

With given  $(\mathbf{x}, \mathbf{y})$ , sub-problem 3 can be expressed as

$$\begin{aligned} \max_{\mathbf{q}} \quad & \sum_{n=1}^N [\log_2(1 + a_n q[n]) - \log_2(1 + bq[n])] \\ \text{s.t.} \quad & (10), \end{aligned} \tag{29}$$

where  $a_n$  is defined in (18) and

$$b = \frac{\gamma_0}{L^\kappa}. \tag{30}$$

Problem (29) is similar to sub-problem 1 given in (17), thus it can be solved by using (20) and (21), provided that  $b_n$  in (20) and (21) is replaced with  $b$  in (30).



### B. Sub-Problem 4: Optimizing UAV Trajectory Given Transmit Power

With given  $\mathbf{q}$ , by letting  $Q_n = \gamma_0 q[n]$  and removing the terms in the objective function in (28) which are irrelevant to  $\mathbf{x}$  and  $\mathbf{y}$ , we express sub-problem 4 as

$$\begin{aligned} \max_{\mathbf{x}, \mathbf{y}} \quad & \sum_{n=1}^N \log_2 \left( 1 + \frac{Q_n}{x^2[n] + y^2[n] + H^2} \right) \\ \text{s.t.} \quad & (1). \end{aligned} \quad (31)$$

Unlike sub-problem 2 given in (22) for the U2G case, problem (31) is simplified as maximizing only the average achievable rate from the ground node to the UAV. This is because the trajectory of the UAV determines only the channel gain from the ground node to the UAV, but does not have any effect on the channel from the ground node to the eavesdropper.

Despite the non-convexity of problem (31), we apply the successive convex optimization to approximately solve it, similar to problem (22). First, we introduce slack variable  $\mathbf{u} = [u[1], \dots, u[N]]^\dagger$ , and solve the following problem which has the same optimal solution of  $(\mathbf{x}, \mathbf{y})$  as problem (31),

$$\max_{\mathbf{x}, \mathbf{y}, \mathbf{u}} \quad \sum_{n=1}^N \log_2 \left( 1 + \frac{Q_n}{u[n]} \right) \quad (32a)$$

$$\text{s.t.} \quad x^2[n] + y^2[n] + H^2 - u[n] \leq 0, \quad \forall n, \quad (32b)$$

$$(1).$$

With a given initial point  $\mathbf{u}_{\text{fea}} \triangleq [u_{\text{fea}}[1], \dots, u_{\text{fea}}[N]]^\dagger$ , which is feasible to (32), and by applying the first-order Taylor expansion of  $\log_2 \left( 1 + \frac{Q_n}{u[n]} \right)$  given in (24) (where  $P_n$  is replaced by  $Q_n$ ), problem (32) is recast as

$$\max_{\mathbf{x}, \mathbf{y}, \mathbf{u}} \quad \sum_{n=1}^N -\frac{Q_n u[n]}{\ln 2 (u_{\text{fea}}^2[n] + Q_n u_{\text{fea}}[n])} \quad (33)$$

$$\text{s.t.} \quad (1), (32b).$$

It can be shown that problem (33) is a convex quadratically constrained quadratic programming (QCQP) problem, and thus can be efficiently solved by the interior-point method [31]. The details of the overall algorithm for solving (P2) are omitted for brevity, given the similarity to that for (P1).

## V. SIMULATION RESULTS

In this section, we provide simulation results to verify the performance of our proposed joint UAV trajectory optimization and transmit power control algorithm (denoted as “joint traj. opt. & pow. ctrl.”). For comparison, we also consider the following three benchmark schemes without optimized trajectory and/or power control:

- Trajectory optimization without transmit power control (denoted as “traj. opt. w/o pow. ctrl.”);
- Best-effort trajectory design with transmit power control (denoted as “best-effort traj. w/ pow. ctrl.”);
- Best-effort trajectory design without transmit power control (denoted as “best-effort traj. w/o pow. ctrl.”).

Specifically, the “traj. opt. w/o pow. ctrl.” algorithm designs the UAV trajectories for the U2G and G2U cases by solving problems (27) and (33) iteratively until convergence, respectively, with transmit power equally set over time, i.e.,  $p[n] = \bar{P}$  and  $q[n] = \bar{Q}$ ,  $\forall n$ . Both the “best-effort traj. w/ pow. ctrl.” and “best-effort traj. w/o pow. ctrl.” algorithms design the UAV trajectories in the following heuristic best-effort manner: the UAV first flies straight to the point above the ground node at its maximum speed, then remains static at that point (if time permits), and finally flies at its maximum speed to reach its final location by the end of the last time slot. Note that if the UAV does not have sufficient time to reach the point above the ground node, it will turn at a certain midway point and then fly to the final location at the maximum speed. Given this trajectory, the “best-effort traj. w/ pow. ctrl.” algorithm optimizes the transmit power in the U2G or G2U case by solving problem (17) or (29), respectively; while the “best-effort traj. w/o pow. ctrl.” algorithm sets transmit power equally over time, i.e.,  $p[n] = \bar{P}$  and  $q[n] = \bar{Q}$ ,  $\forall n$ . The initial feasible solutions for the proposed “joint traj. opt. & pow. ctrl.” and benchmark “traj. opt. w/o pow. ctrl.” algorithms are generated by the “best-effort traj. w/o pow. ctrl.” algorithm.

The distance between the ground node and the eavesdropper is set as  $L = 200\text{m}$ , and the flying altitude of the UAV is set as  $H = 100\text{m}$ . The maximum speed of the UAV is  $v_{\max} = 3\text{m/s}$ . The flight time  $T$  is divided into multiple time slots with equal length of  $d_t = 0.5\text{s}$ . The communication bandwidth is 20MHz with the carrier frequency at 5GHz, and the noise power spectrum density is  $-169\text{dBm/Hz}$ . Thus, the reference SNR at the reference distance  $d_0 = 1\text{m}$  is  $\gamma_0 = 80\text{dB}$ . The peak transmit power limits for the U2G and G2U links are set as  $P_{\text{peak}} = 4\bar{P}$

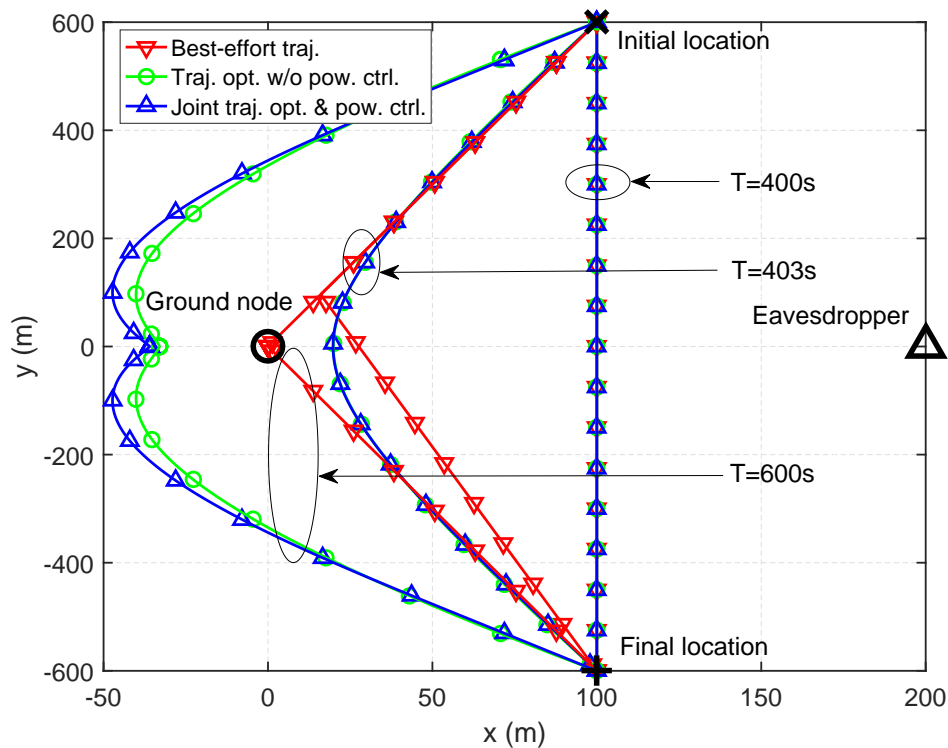


Fig. 2. Trajectories of the UAV for the U2G communication in Case 1.

and  $Q_{\text{peak}} = 4\bar{Q}$ , respectively. The threshold in Algorithm 1 is set as  $\epsilon = 10^{-4}$ . We consider two cases, denoted as Case 1 and Case 2, in which the UAV has different initial and final locations. In Case 1, the UAV's initial and final locations are on the vertical line in the middle of the ground node and the eavesdropper, and the coordinates of them are set as  $(x_0, y_0) = (100, 600)\text{m}$  and  $(x_F, y_F) = (100, -600)\text{m}$ , as shown in Fig. 2. In Case 2, the UAV's initial and final locations are on the parallel line of that connecting the ground node and the eavesdropper, and the coordinates of them are set as  $(x_0, y_0) = (-500, -150)\text{m}$  and  $(x_F, y_F) = (700, -150)\text{m}$ , as shown in Figs. 5 and 8.

#### A. U2G Communication

In the U2G case, we first consider Case 1. Fig. 2 shows the trajectories of the UAV by applying different algorithms with different values of flight time  $T$ . The average transmit power is set as  $\bar{P} = -5\text{dBm}$ . The locations of the ground node, eavesdropper, as well as the UAV's initial and final locations are marked with  $\circ$ ,  $\triangle$ ,  $\times$ , and  $+$ , respectively. It is observed that when

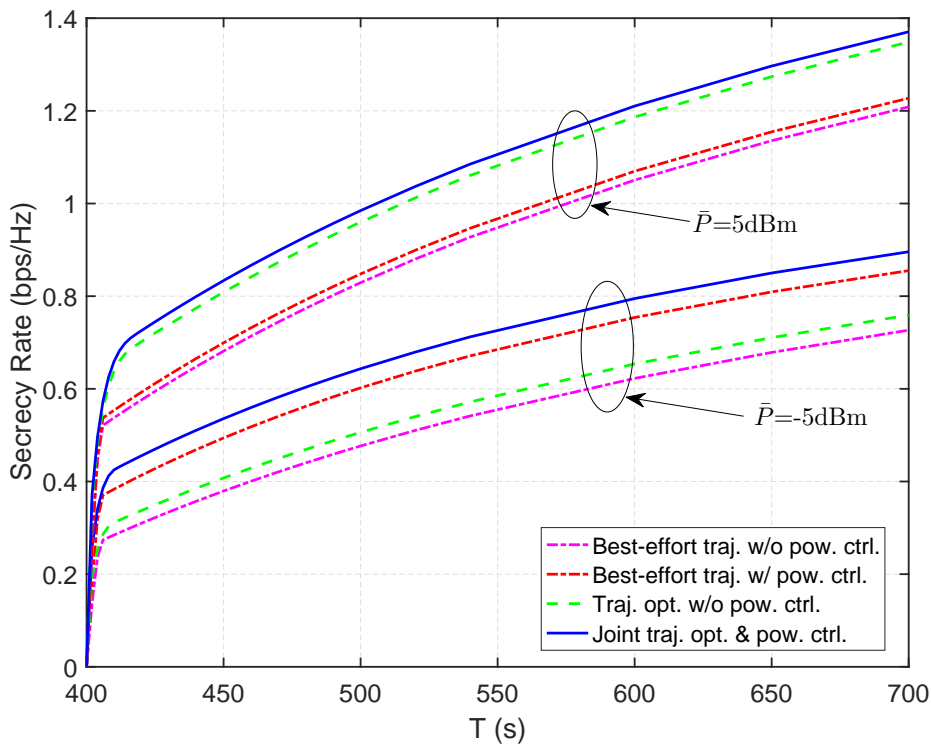


Fig. 3. Secrecy rate versus flight time  $T$  for the U2G communication in Case 1.

$T = 400$ s which is the minimum time required for the UAV to fly from the initial location to the final location in a straight line at the maximum speed, the trajectories of all algorithms are identical. As  $T$  increases, the trajectories by the proposed “joint traj. opt. & pow. ctrl.” and the benchmark “traj. opt. w/o pow. ctrl.” are still similar, i.e., the UAV tries to fly as close as possible to the ground node and at the same time as far away as possible to the eavesdropper, while they appear different compared to that by the heuristic best-effort trajectory design (same for with and without power control). When  $T$  is sufficiently large, i.e.  $T = 600$ s, for the proposed “joint traj. opt. & pow. ctrl.” or the benchmark “traj. opt. w/o pow. ctrl.”, it is observed that the UAV first flies at the maximum speed to reach a certain location on the left of the ground node (not directly above it), then remains stationary at this location as long as possible, and finally flies to the final location in an arc path at the maximum speed and reaches there by the end of the last time slot. These stationary locations, which are on the opposite direction of the eavesdropper, strike an optimal balance between enhancing the legitimate link channel and degrading the eavesdropping link channel and hence maximize the secrecy rate in each of these

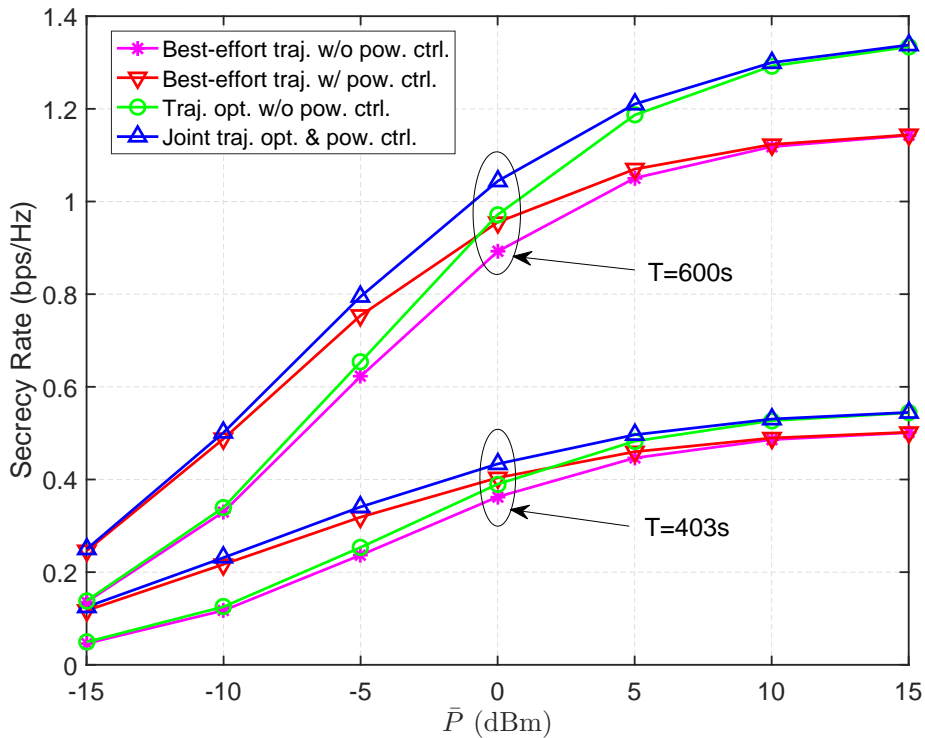


Fig. 4. Secrecy rate versus average transmit power  $\bar{P}$  for the U2G communication in Case 1.

two cases. In fact, this is also why the UAV follows an arc path rather than the straight path as in the heuristic best-effort trajectory.

Fig. 3 shows the corresponding average secrecy rates of different algorithms versus flight time  $T$  when  $\bar{P} = -5\text{dBm}$  and  $5\text{dBm}$ . It is observed that the secrecy rates of all algorithms increase significantly with  $T$ . This is because for all algorithms the maximum secrecy rate is achieved at their respective stationary locations (see Fig. 2) for sufficiently large  $T$ , and larger  $T$  results in longer hovering time at such locations for the UAV. The proposed “joint traj. opt. & pow. ctrl.” algorithm always achieves the highest secrecy rate, while the benchmark “best-effort traj. w/o pow. ctrl.” algorithm has the lowest secrecy rate, as expected. When  $\bar{P} = -5\text{dBm}$ , the benchmark “best-effort traj. w/ pow. ctrl.” algorithm has higher secrecy rate than that of the benchmark “traj. opt. w/o pow. ctrl.” algorithm. In contrast, when  $\bar{P} = 5\text{dBm}$ , the latter algorithm has higher secrecy rate than the former. Such results suggest that in the low transmit power regime, power control is more important for improving the secrecy rate; while in the high transmit power regime, trajectory optimization is more significant. Furthermore, it is worth pointing out that trajectory

adaptation with increasing  $T$  is essential for the secrecy rate improvement, even for the case with heuristic best-effort trajectory. Otherwise, if the trajectory is fixed (e.g., following the straight line from the initial to final location with constant speed of  $\sqrt{(x_F - x_0)^2 + (y_F - y_0)^2}/T$  regardless of  $T$ , then the secrecy rate will remain unchanged as the case with required minimum  $T = 400$ s in Fig. 3, i.e., the UAV cannot exploit its mobility to improve the secrecy rate, even with sufficiently large  $T$ .

Fig. 4 shows the average secrecy rates of different algorithms versus the average transmit power  $\bar{P}$  when  $T = 403$ s and  $600$ s. It is observed that the proposed “joint traj. opt. & pow. ctrl.” algorithm always achieves the highest secrecy rate, while the benchmark “best-effort traj. w/o pow. ctrl.” algorithm has the lowest secrecy rate. In addition, when  $\bar{P} \leq -5$ dB, we note that the benchmark “best-effort traj. w/ pow. ctrl.” algorithm achieves a secrecy rate performance close to the proposed “joint traj. opt. & pow. ctrl.” algorithm, and also significantly outperforms the benchmark “traj. opt. w/o pow. ctrl.” algorithm. However, when  $\bar{P}$  increases, the secrecy rate of the benchmark “traj. opt. w/o pow. ctrl.” algorithm will eventually exceed that of the benchmark “best-effort traj. w/ pow. ctrl.” algorithm and even get closer to that of the proposed “joint traj. opt. & pow. ctrl.” algorithm. Furthermore, the rate gap between the benchmark “traj. opt. w/o pow. ctrl.” and benchmark “best-effort traj. w/ pow. ctrl.” becomes larger with increasing  $\bar{P}$ . The above results further demonstrate that transmit power control is more effective in improving secrecy rate than trajectory optimization when the average transmit power is low, while trajectory optimization is more effective when the average transmit power is high.

Next, we consider Case 2. Fig. 5 shows the trajectories of the UAV by using different algorithms when  $\bar{P} = -5$ dBm. It is observed that different from the results in Case 1 shown in Fig. 2, the trajectories by the proposed “joint traj. opt. & pow. ctrl.” and benchmark “traj. opt. w/o pow. ctrl.” algorithms with  $T = 405$ s or  $600$ s differ significantly, especially when the UAV flies towards the final location. For the proposed algorithm, the UAV flies along a relatively direct path towards the ground node and then towards the final location. In contrast, for this benchmark, the UAV first flies almost directly to the ground node, but then flies along an arc path to the final location, which inevitably consumes more time on the traveling compared to the proposed trajectory. The reason for such a difference is that in Case 2, flying from the ground node towards the final location reduces the distance from the UAV to the eavesdropper less much as compared to that from it to the ground node, which is undesired. This means that to improve the secrecy rate, the UAV should reduce transmit power when it gets farther away

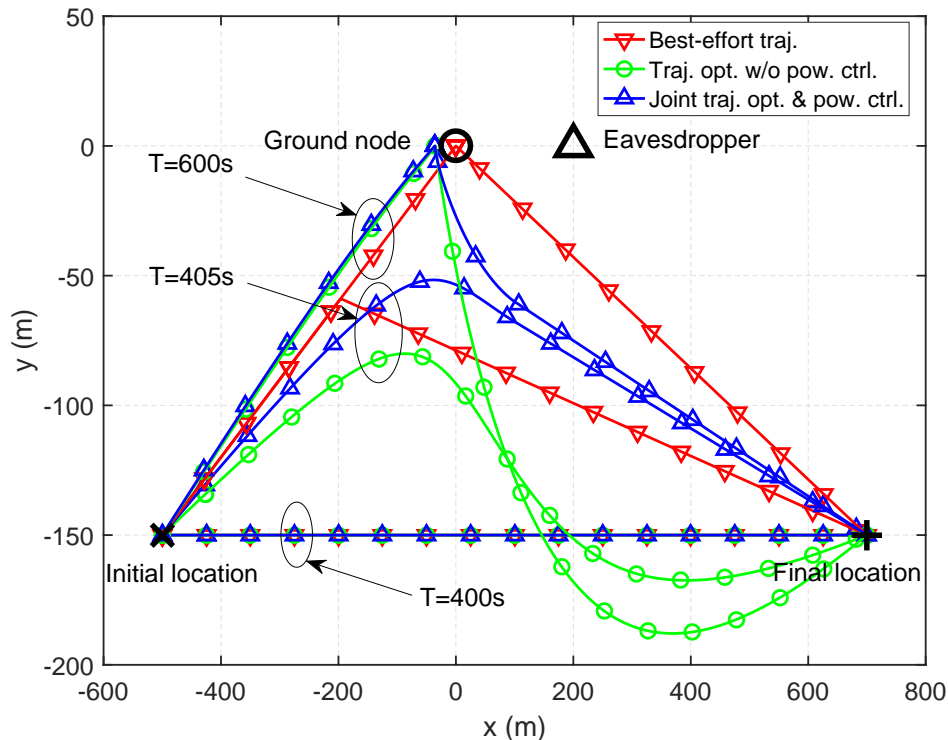


Fig. 5. Trajectories of the UAV for the U2G communication in Case 2.

from the ground node and closer to the final location. Considering this fact, the proposed “joint traj. opt. & pow. ctrl.” algorithm is able to decrease the UAV transmit power or even turn off the transmitter to save power and also protect from eavesdropping when the UAV flies directly towards the final location. However, for the benchmark “traj. opt. w/o pow. ctrl.” algorithm that employs a constant transmit power, the UAV can only rely on adjusting its trajectory to keep far away from the eavesdropper to avoid being eavesdropped, which however requires more traveling time and leads to a longer arc trajectory.

With such a UAV trajectory difference, the secrecy rate performances of different algorithms versus  $T$  and  $\bar{P}$ , which are shown in Figs. 6 and 7 respectively, are also quite different from those shown in Figs. 3 and 4 for Case 1. Specifically, the secrecy rate gaps between the proposed “joint traj. opt. & pow. ctrl.” and benchmark “traj. opt. w/o pow. ctrl.” algorithms versus  $T$  or  $\bar{P}$  in Case 2 are significantly larger than those in Case 1. For example, in Fig. 6, the “traj. opt. w/o pow. ctrl.” algorithm even has lower secrecy rate than the “best-effort traj. w/o pow. ctrl.” algorithm in the regime of  $T \leq 650s$  when  $\bar{P} = -5dBm$  or in the regime of  $T \leq 550s$  when

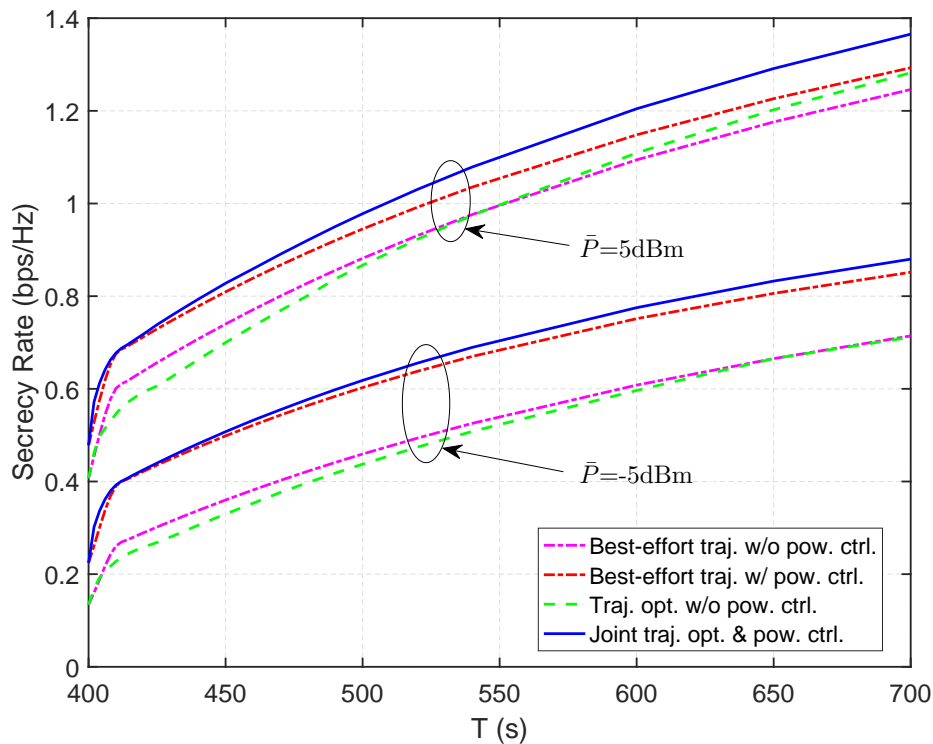


Fig. 6. Secrecy rate versus flight time  $T$  for the U2G communication in Case 2.

$\bar{P} = 5\text{dBm}$ . In addition, in Fig. 7, the “traj. opt. w/o pow. ctrl.” algorithm has a lower secrecy rate than the “best-effort traj. w/o pow. ctrl.” algorithm over the whole  $\bar{P}$  regime when  $T = 405\text{s}$  and in the regime of  $\bar{P} \leq 0\text{dBm}$  when  $T = 600\text{s}$ . This is mainly because the UAV wastes more time on travelling along a longer arc trajectory to reach the final location which in turn leads to the inefficient use of the transmit power. The above results demonstrate the importance and necessity of the joint UAV trajectory optimization and transmit power control in maximizing the secrecy rate for U2G communication.

### B. G2U Communication

In the G2U case, the channel gain from the ground node to the eavesdropper given in (9) contains a small-scale Rayleigh fading term  $\zeta$ . Thus, all secrecy rate results in the following are averaged over 5000 random independent realizations of  $\zeta$ , where the path-loss exponent is set as  $\kappa = 3$ . Since our results obtained for Cases 1 and 2 lead to consistent observations, we only present the results for Case 2 due to the space limitation.



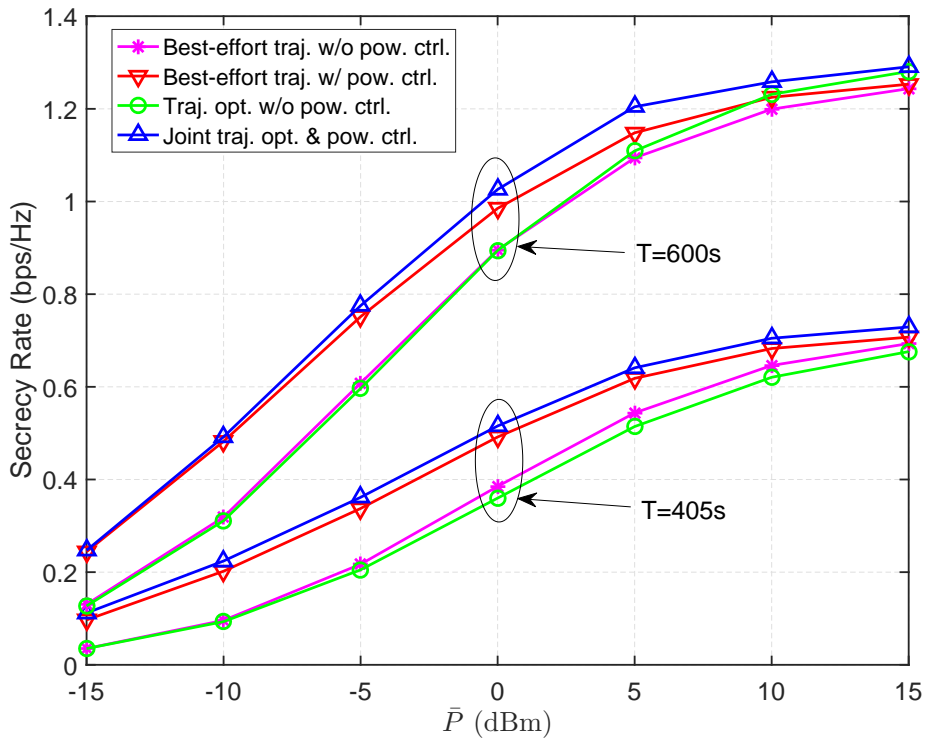


Fig. 7. Secrecy rate versus average transmit power  $\bar{P}$  for the U2G communication in Case 2.

Fig. 8 shows the trajectories of the UAV with different values of  $T$  when the average transmit power is  $\bar{Q} = -5\text{dBm}$ . It is observed that the trajectories of the proposed “joint traj. opt. & pow. ctrl.” and benchmark “traj. opt. w/o pow. ctrl.” algorithms are very similar for different values of  $T$ , i.e., the UAV tries to fly as close as possible to the ground node as  $T$  increases. When  $T$  is sufficiently large, i.e.,  $T = 600\text{s}$ , the trajectories of them are the same as the heuristic best-effort trajectory, i.e., the UAV first flies at the maximum speed to reach the point right above the ground node, then remains static as long as possible, and finally flies to the final location directly at the maximum speed in order to reach there by the end of the last time slot. The fundamental reason of such a result is that in the G2U setup, the channel between the ground node (transmitter) and the eavesdropper is independent of the UAV’s location. Therefore, the UAV trajectory is only optimized to maximize achievable rate from the ground node to the UAV. Obviously, the point right above the ground node is the best location for achieving its largest rate. This explains why the optimized trajectory also converges to the heuristic best-effort trajectory when  $T$  is sufficiently large.

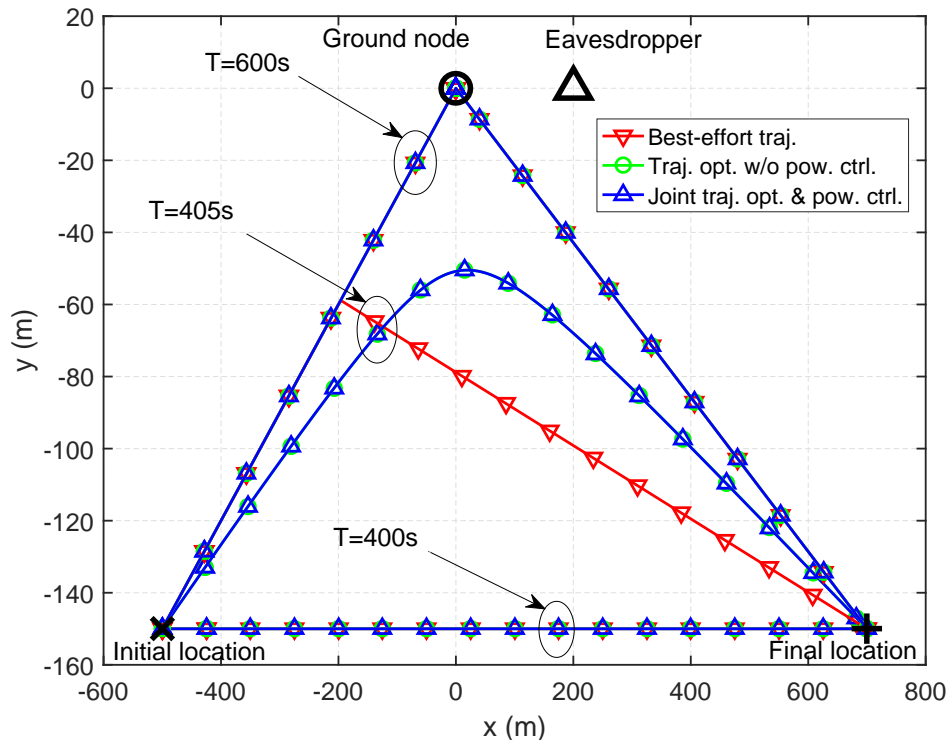


Fig. 8. Trajectories of the UAV for the G2U communication in Case 2.

Fig. 9 shows the average secrecy rates of different algorithms versus flight time  $T$  when  $\bar{Q} = -5\text{dBm}$  and  $5\text{dBm}$ . When  $T \geq 410\text{s}$ , the algorithms with transmit power control, i.e. the proposed “joint traj. opt. & pow. ctrl.” and benchmark “best-effort traj. w/ pow. ctrl.” algorithms, achieve the same secrecy rate since they have the same trajectory and hence the same transmit power control, while they both outperform the benchmark algorithms without power control, i.e., the “traj. opt. w/o pow. ctrl.” and “best-effort traj. w/o pow. ctrl.” algorithms. These results suggest that transmit power control is more effective than trajectory optimization in improving secrecy rate in the G2U case, as shown in Fig. 8, since the optimal trajectory can be easily achieved by the heuristic best-effort design when  $T$  is sufficiently large. Furthermore, the secrecy rate gap between the algorithms with and without power control when  $\bar{Q} = -5\text{dBm}$  is significantly larger than that when  $\bar{Q} = 5\text{dBm}$ , since power control is more effective when the average transmit power is low.

Fig. 10 shows the average secrecy rates of different algorithms versus average transmit power  $\bar{Q}$  when  $T = 405\text{s}$  and  $600\text{s}$ . It can be also observed that transmit power control is effective for

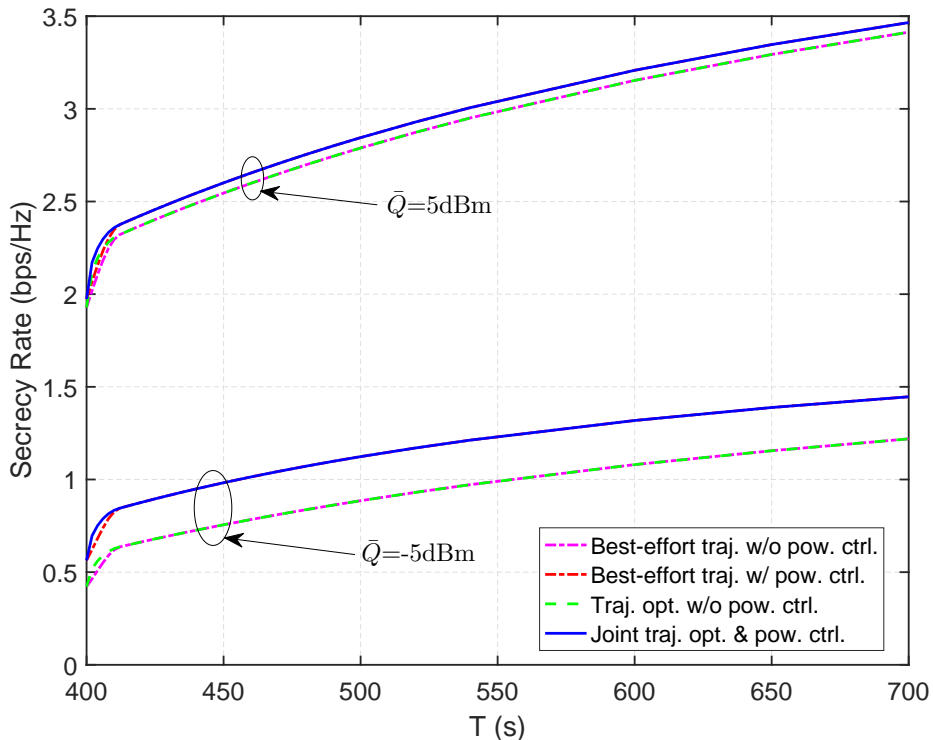


Fig. 9. Secrecy rate versus flight time  $T$  for the G2U communication in Case 2.

improving secrecy rate when  $\bar{Q} \leq 0\text{dBm}$ . When  $T = 405\text{s}$ , the secrecy rate gap between the proposed “joint traj. opt. & pow. ctrl.” algorithm and the benchmark algorithms with best-effort trajectory exists due to their trajectory difference. When  $T = 600\text{s}$ , the secrecy rates of all algorithms tend to be very similar when  $\bar{Q} \geq 10\text{dBm}$ . This is because their trajectories are the same and the power control only provides marginal rate gain when transmit power is high.

## VI. CONCLUSION

In this paper, we study the PHY layer security for emerging UAV communications in the forthcoming 5G wireless networks. Specifically, we propose to enhance the security performance by proactively controlling channel gains via adjusting the UAV trajectory in addition to applying the conventional power/rate adaptation, which leads to a new joint optimization framework. For both the U2G and G2U communications, the transmit power control and UAV trajectory are jointly designed to maximize the average secrecy rate over a finite horizon, subject to the average and peak transmit power constraints as well as practical UAV’s mobility constraints.

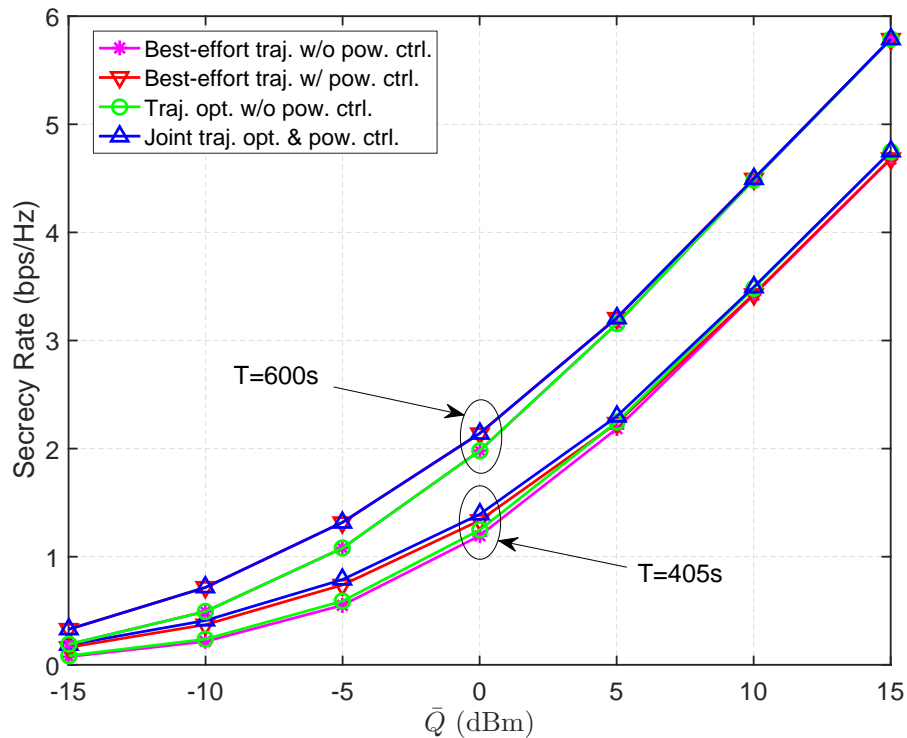


Fig. 10. Secrecy rate versus average transmit power  $\bar{Q}$  for the G2U communication in Case 2.

By applying the block coordinate descent and successive convex optimization methods, efficient iterative algorithms are proposed to solve the joint design problems. Simulation results show that joint trajectory optimization and transmit power control improves the PHY layer security performance, and more significantly in the U2G case compared to the G2U case, as the UAV trajectory in the U2G case has an effect on both the legitimate and eavesdropping channels, instead of the legitimate channel only in the G2U case. Furthermore, it is found that both UAV trajectory optimization and transmit power control are generally necessary in the U2G case; while in the G2U case, transmit power control is more effective than UAV trajectory optimization for improving the secrecy rate performance, and the heuristic best-effort trajectory already performs quite close to the optimized trajectory.

## REFERENCES

- [1] G. Zhang, Q. Wu, M. Cui, and R. Zhang, "Securing UAV communications via trajectory optimization," in *Proc. IEEE GLOBECOM*, Dec. 2017, [Online]. Available: <https://arxiv.org/abs/1710.04389>.

- [2] Y. Zeng, R. Zhang, and T. J. Lim, "Wireless communications with unmanned aerial vehicles: opportunities and challenges," *IEEE Commun. Mag.*, vol. 54, no. 5, pp. 36-42, May 2016.
- [3] "Paving the path to 5G: optimizing commercial LTE networks for drone communication," [Online]. Available: <https://www.qualcomm.com/news/onq/2016/09/06/paving-path-5g-optimizing-commercial-lte-networks-drone-communication>.
- [4] "Ericsson and China Mobile conduct world's first 5G drone prototype field trial," [Online]. Available: <https://www.ericsson.com/en/news/2016/8/ericsson-and-china-mobile-conduct-worlds-first-5g-drone-prototype-field-trial->.
- [5] Q. Wu and R. Zhang, "Common throughput maximization in UAV-enabled OFDMA systems with delay consideration," *submitted to IEEE Trans. Commun.*, 2017, [Online] Available: <https://arxiv.org/abs/1801.00444>
- [6] M. Mozaffari, W. Saad, M. Bennis, and M. Debbah, "Drone small cells in the clouds: design, deployment and performance analysis," in *Proc. IEEE GLOBECOM*, Dec. 2015.
- [7] R. I. Bor-Yaliniz, A. El-Keyi, and H. Yanikomeroglu, "Efficient 3-D placement of an aerial base station in next generation cellular networks," in *Proc. IEEE ICC*, May 2016.
- [8] J. Lyu, Y. Zeng, R. Zhang, and T. J. Lim, "Placement optimization of UAV-mounted mobile base stations," *IEEE Commun. Lett.*, vol. 21, no. 3, pp. 604-607, Mar. 2017.
- [9] Q. Wu, Y. Zeng, and R. Zhang, "Joint trajectory and communication design for UAV-enabled multiple access," in *IEEE Global Communications Conference (GLOBECOM)*, Dec. 2017.
- [10] Q. Wu, Y. Zeng, and R. Zhang, "Joint trajectory and communication design for multi-UAV enabled wireless networks," *IEEE Trans. Wireless Commun.*, 2017, [Online] Available: <http://ieeexplore.ieee.org/document/8247211/>.
- [11] V. Sharma, M. Bennis, and R. Kumar, "UAV-assisted heterogeneous networks for capacity enhancement," *IEEE Commun. Lett.*, vol. 20, no. 6, pp. 1207-1210, Jun. 2016.
- [12] Y. Zeng, R. Zhang, and T. J. Lim, "Throughput maximization for UAV-enabled mobile relaying systems," *IEEE Trans. Commun.*, vol. 64, no. 12, pp. 4983-4996, Dec. 2016.
- [13] T. A. Johansen, A. Zolich, T. Hansen, and A. J. Sørensen, "Unmanned aerial vehicle as communication relay for autonomous underwater vehicle – field tests," in *IEEE Globecom Commun. Conf. Workshops*, pp. 1469-1474, Dec. 2014.
- [14] S. Sotheara, K. Aso, N. Aomi, and S. Shimamoto, "Effective data gathering and energy efficient communication protocol in wireless sensor networks employing UAV," in *Proc. IEEE WCNC*, pp. 2342-2347, 2014.
- [15] J. Lyu, Y. Zeng, and R. Zhang, "Cyclical multiple access in UAV-aided communications: a throughput-delay tradeoff," *IEEE Wireless Commun. Lett.*, vol. 5, no. 6, pp. 600-603, Dec. 2016.
- [16] "Cellular enables safer drone deployments," [Online]. Available: <https://www.qualcomm.com/invention/technologies/lte/advanced-pro/cellular-drone-communication>.
- [17] N. H. Motlagh, M. Baggaa, and T. Taleb, "UAV-based IoT platform: a crowd surveillance use case," *IEEE Commun. Mag.*, vol. 55, no. 2, pp. 128-134, Feb. 2017.
- [18] P. K. Gopala, L. Lai, and H. E. Gamal, "On the secrecy capacity of fading channels," *IEEE Trans. Inf. Theory*, vol. 54, no. 10, pp. 4687-4698, Oct. 2008.
- [19] Y. Liang, H. V. Poor, and S. Shamai, "Secure communication over fading channels," *IEEE Trans. Inf. Theory*, vol. 54, no. 6, pp. 2470-2492, Jun. 2008.
- [20] X. Wang, M. Tao, J. Mo, and Y. Xu, "Power and subcarrier allocation for physical-layer security in OFDMA-based broadband wireless networks," *IEEE Trans. Inf. Forensics Security*, vol. 6, no. 3, pp. 693-702, Sep. 2011.
- [21] H. Xing, L. Liu, and R. Zhang, "Secrecy wireless information and power transfer in fading wiretap channel," *IEEE Trans. Veh. Technol.*, vol. 65, no. 1, pp. 180-190, Jan. 2016.

- [22] A. Khisti and G. W. Wornell, "Secure transmission with multiple antennas—part II: the MIMOME wiretap channel," *IEEE Trans. Inf. Theory*, vol. 56, no. 11, pp. 5515-5532, Nov. 2010.
- [23] Y. Wu, C. Xiao, Z. Ding, X. Gao, and S. Jin, "Linear precoding for finite-alphabet signaling over MIMOME wiretap channels," *IEEE Trans. Veh. Technol.*, vol. 61, no. 6, pp. 2599-2612, Jul. 2012.
- [24] G. Zheng, L. C. Choo, and K. K. Wong, "Optimal cooperative jamming to enhance physical layer security using relays," *IEEE Trans. Signal Process.*, vol. 59, no. 3, pp. 1317-1322, Mar. 2011.
- [25] Y. Zou, X. Wang, and W. Shen, "Physical-layer security with multiuser scheduling in cognitive radio networks," *IEEE Trans. Commun.*, vol. 61, no. 12, pp. 5103-5113, Dec. 2013.
- [26] M. Erdelj, E. Natalizio, K. R. Chowdhury, and I. F. Akyildiz, "Help from the sky: leveraging UAVs for disaster management," *IEEE Pervasive Comput.*, vol. 16, no. 1, pp. 24-32, Jan. 2017.
- [27] M. Caris, et al., "mm-Wave SAR demonstrator as a test bed for advanced solutions in microwave imaging," *IEEE Aerosp. Electron. Syst. Mag.*, vol. 29, no. 7, pp. 8-15, Jul. 2014.
- [28] F. Jiang and A. L. Swindlehurst, "Optimization of UAV heading for the ground-to-air uplink," *IEEE J. Sel. Areas Commun.*, vol. 30, no. 5, pp. 993-1005, Jun. 2012.
- [29] Y. Zeng and R. Zhang, "Energy-efficient UAV communication with trajectory optimization," *IEEE Trans. Wireless Commun.*, vol. 16, no. 6, pp. 3747-3760, Jun. 2017.
- [30] X. Lin, et al., "The sky is not the limit: LTE for unmanned aerial vehicles," [Online]. Available: <https://arxiv.org/pdf/1707.07534>.
- [31] S. Boyd and L. Vandenberghe, *Convex Optimization*. Cambridge University Press, 2004.